

# Global Internet public peering capacity of interconnection: a complex network analysis

Justin Loye

IRIT, LPT, Université de Toulouse  
CNRS, Toulouse INP, UT3  
Toulouse, France  
justin.loye@irit.fr

Sandrine Mouysset  
IRIT, Université de Toulouse  
CNRS, Toulouse INP, UT3  
Toulouse, France  
sandrine.mouysset@irit.fr

Marc Bruyère  
IIJ, University of Tokyo,  
CNRS IRL 3527  
Tokyo, Japan  
mbruyere@nc.u-tokyo.ac.jp

Katia Jaffrès-Runser  
IRIT, Université de Toulouse  
CNRS, Toulouse INP, UT3  
Toulouse, France  
katia.jaffres-runser@irit.fr

June 13, 2022

## Abstract

A massive and growing part of Autonomous System (AS)-level traffic exchanges takes place at Internet Exchange Points (IXPs). This paper leverages PeeringDB, a database providing a partial but reasonable view of the global interconnection of ASes at IXPs, to model a complex graph enabling the characterization of the key Internet peering players and their interactions over time. We model a PeeringDB snapshot as a weighted directed bipartite graph, called the *pDB c-graph*, that captures the port size ASes possess at IXPs using available metadata. This novel model of the Internet is shown to picture relevant features of a complex network that groups ASes and IXPs in geographical areas of influence. From this model, we extract central players of public peering such as hypergiant AS content providers and major regional traffic receivers. Most importantly, this graph model opens the way to apply spectral analysis using reduced Google matrix in order to retrieve the intensity of possible interactions between ASes on the basis of pure connectivity information. As an illustration, we retrieve the timely evolution of the peering network to show

how the central content and cloud providers have increased their reach to eyeball networks during Covid-19 pandemic.

## 1 Introduction

Internet is structured around Autonomous Systems (ASes), administered by Internet Service Providers (ISPs), content providers, universities, etc. They are located all over the world and connect at different Points of Presence (PoPs), either using a pairwise private peering connection or doing public peering in multi-party shared switch fabric known as Internet eXchange Point (IXP). In the early 2000's, most ASes connected through private links, with a customer/provider relationship inducing a hierarchical structure of the Internet. The last decade has seen a surge in the deployment and the growth of IXPs, leading to a flattened Internet topology [1]. This momentum was driven by the more diverse and cheaper interconnection services IXPs offer around the world to reach regional delivery networks. Content providers find in IXPs a chance to reach in a relatively reduced deployment time, sometimes using a tier remote peering service, the regional networks connected to the end users [2]. Fundamental works [3] [4] showcased that IXPs were growing in importance by enabling more and more Internet traffic since the early 2010s. Recent studies showed that IXPs enabled to cope with the network stress caused by end-user increase demand during the Covid-19 outbreak [5] [6].

Thus, knowledge of the public peering ecosystem and its underlying graph structure is a key element of understanding the global Internet topology. However to fully grasp the AS interconnections, one would need to obtain a traffic matrix for each IXP. Such traffic matrices are not publicly disclosed, and only a few have been described in the scientific literature in recent years [7] [8] [3]. To the best of our knowledge, the most comprehensive source of AS-level topology data is Caida's AS relationships [9]. This dataset labels AS relationships as "customer-to-provider" and "peer-to-peer". However peer-to-peer inference is notoriously hard and Caida's work, while invaluable to the research community, is known to miss most of those links. On the other hand, the authoritative source of information regarding public peering ecosystem is PeeringDB, a community database where ASes register their own information and IXP membership in order to find new peers. This IXP membership is best described by an unweighted and undirected bipartite AS-IXP graph [10], but such a graph does contain direct links between ASes and information about traffic exchanges.

To circumvent these problems, in this paper we define a weighted oriented bipartite graph model of the Internet based on PeeringDB. We leverage the router `port.size` that ASes have at IXPs to peer with other IXP participants. Actual traffic between ASes is not available, but we have an `AS.info_ratio` attribute that indicates the general tendency to receive or send traffic. We show that this bipartite graph has shared characteristics across complex networks and is expressive enough to encode the main features of the global peering ecosystem. With a novel spectral graph theory approach based on stochastic complemen-

tation from Markov chain theory [11], we leverage the graph to approximate AS-AS traffic exchanges at a global scale. This new PeeringDB model allows us to make the following contributions:

- identify the main sources of Internet traffic known as “hypergiants”,
- extract the regional presence of ASes from the structural properties,
- identify the main traffic destinations as regional ISPs close to the end-user, known as “eyeball networks”,
- study the diffusion patterns of hypergiants to regional ISPs with spectral graph theory,
- illustrate the model on a longitudinal study of the Covid-19 demand for content.

The rest of the paper is organized as follows. We start by presenting PeeringDB in section 2. We then introduce our graph model in section 3 and perform an analysis of its main features in section 4. In section 5, we introduce a graph theory tool known as stochastic complementation [11] to study the hypergiants diffusion to eyeball networks. Lastly, we show in section 6 how hypergiants reacted to the demand increase from end-users during Covid-19 outbreak.

All processed data, source codes and network visualisation files will be made available [12] for final publication.

## 2 PeeringDB

PeeringDB<sup>1</sup> is a non-profit and user-maintained database that facilitates the global interconnection of networks at IXPs, data centers, and other interconnection facilities. Network operators register information about their organisation, networks and point of presence, creating a picture of the peering ecosystem. From this picture, network operators are able to identify new potential peers and how to choose the best PoP to expand their network. As of 2022, 12689 registered ASes reports presence at IXPs. In total, there are 872 IXPs reporting members, of which 771 have at least 3 participants and can thus be used for multilateral traffic exchange. PeeringDB can be accessed publicly with an API, and daily dumps are made available to the community by Caida from 2010 to the present day [13].

PeeringDB is recognized as an authoritative source of information. Most of the data is now uploaded automatically using IXP management software. For instance, small to medium size IXPs generally deploy *IXP Manager*<sup>2</sup> which is currently used by 184 IXPs. Larger IXPs have as well automated PeeringDB declarations in their in-house management software through the PeeringDB API. As such, network operators can use PeeringDB as part of their

---

<sup>1</sup><https://www.peeringdb.com/>

<sup>2</sup><https://www.ixpmanager.org/>

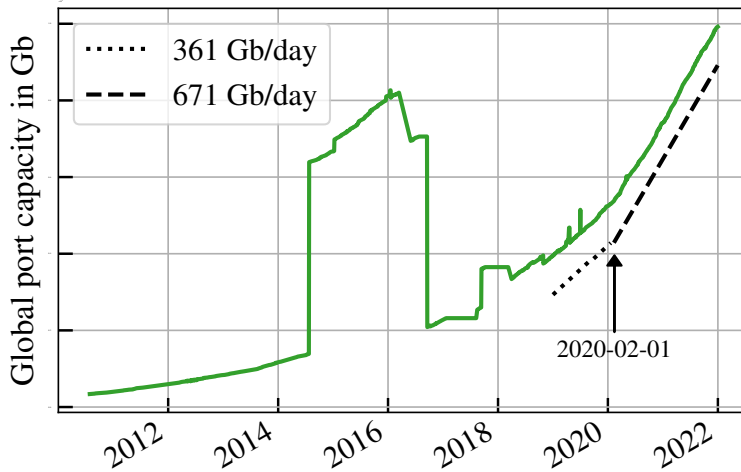


Figure 1: Daily evolution of the total port capacity of ASes of PeeringDB between 2010-07-29 and 2021-12-31. *An inflection point in 2020-02 is underlined by two linear regressions with respective slope of 361 and 671 Gbit/day.*

automation process. It is in an organisation’s best interest to have an accurate and updated record. PeeringDB has been validated by BGP data in [13], where authors show that PeeringDB membership is generally up-to-date and reasonably representative of the Internet’s transit, content and access providers in terms of business types and geography of participants. Following a more recent study from [2], we argue that PeeringDB can be used as a ground-truth source of data of the publicly declared part of the Internet.

In this paper, we will make use of the port sizes ASes possess at IXPs, reported in PeeringDB, indicating an upper bound to the actual real-time transit taking place between ASes. The sum of all port sizes called port capacity, computed for each AS, has been shown to be a discriminating feature to identify hypergiants ASes [2]. The present work focuses on ASes and IXPs data contained in PeeringDB snapshots collected between 2019-01-01 and 2021-03-01. Before this period, snapshots are more prone to discrepancies that are reflected as outliers in port capacity. The most striking example, also reported in another study [14], is the 2014-2016 bump in global port capacity presented in Figure 1. This bump was caused by a single Australian AS, connected at 5 IXPs, that reported port sizes one hundred times bigger than Akamai, a global content delivery network. From 2019-01-01, outliers are fewer and do not persist over time, indicating efforts in data curation by PeeringDB. In the following, we made sure that the snapshots we are building our conclusions on are not impacted by outliers.

Table 1: Proportions of ASes in size and `port_capacity` for `info_ratio` categories.

<code>info_ratio</code> Categories	<code>port_capacity</code> Proportion (%)	Count Proportion (%)
Balanced (B)	26.12	31.69
Heavy Inbound (HI)	4.72	6.80
Heavy Outbound (HO)	19.68	3.68
Mostly Inbound (MI)	22.45	30.69
Mostly Outbound (MO)	21.34	10.86
Not Disclosed	5.69	16.28

### 3 A new PeeringDB modelling

ASes membership to IXPs reported in PeeringDB can be naturally represented as a weighted bipartite graph. This allows to take advantage of the powerful tools from graph theory, as we will see in section 5. Motivated by this, we introduce a novel graph model, called the *pDB c-graph*, on the basis of the model defined by Nomikos et al. in [10], but augmented with both weighted and directional edges.

#### 3.1 Graph model

The *pDB c-graph* is constructed as a bipartite graph, where the set of vertices  $\mathcal{V}$  is split between two sets  $\mathcal{A}$  and  $\mathcal{X}$  representing the ASes and IXPs of a PeeringDB snapshot. Edges exist between an AS  $as \in \mathcal{A}$  and an IXP  $ix \in \mathcal{X}$  if  $as$  is a member of  $ix$ . Edges  $\mathcal{E}$  are weighted with the router `port_size` metadata, which is associated to inbound and outbound directions following ASes `info_ratio` metadata. We associate to each undirected edge  $e_{i \leftrightarrow j} \in \mathcal{E}$  a real number  $ps(e_{i \leftrightarrow j})$  corresponding to the `port_size`. If an AS has multiple routers at an IXP, we agglomerate their port size to weight a single link. Since the graph is bipartite,  $ps(e_{i \leftrightarrow j}) = 0, \forall (i, j) \in \mathcal{A} \times \mathcal{A} \vee \forall (i, j) \in \mathcal{X} \times \mathcal{X}$ . The *pDB c-graph* is thus defined as:

**Definition 3.1** (*pDB c-graph*)

$$\mathcal{G} = (\mathcal{E}, \mathcal{V}), \text{ with } \mathcal{V} = \mathcal{A} \cup \mathcal{X}$$

The edges direction is derived from both `port_size` and `info_ratio` metadata as follows. In PeeringDB, each AS is associated with the `info_ratio` label representing the traffic imbalance in its relationship with other IXPs' members. Thus, traffic at an AS can be reported as Heavy Outbound (HO), Mostly Outbound (MO), Balanced (B), Mostly Inbound (MI), Heavy Inbound (HI) or Not Disclosed. Around 83% of ASes have a valid label as presented in Table 1, these ASes representing around 94% of the total `port_capacity`.

We leverage this qualitative information to derive a specific port size value for *directed* inbound and outbound edges. Since links are full-duplex, we assume maximum capacity is used by the AS in the direction declared in `info_ratio` label. This hypothesis is reasonable since we model the capacity provisioned by ASes at IXPs and not the real traffic volumes. Therefore, we define a weighted and directed adjacency matrix  $W$ , with elements  $W_{ij}$  indicating a link from  $j$  to  $i$ , the following way:

**Definition 3.2 (Weighted and directed adjacency matrix  $W$ )** *Let  $i \in \mathcal{A}$  and  $j \in \mathcal{X}$ . If  $i$  is registered inbound*

$$W_{ij} = ps(e_{i \leftrightarrow j}), \quad W_{ji} = (1 - \beta) \cdot ps(e_{i \leftrightarrow j}), \quad (1)$$

*and if  $i$  is registered outbound*

$$W_{ij} = (1 - \beta) \cdot ps(e_{i \leftrightarrow j}), \quad W_{ji} = ps(e_{i \leftrightarrow j}), \quad (2)$$

*with a  $\beta \leq 1$  coefficient set for either **Balanced** ( $\beta_B$ ), **Not Disclosed** ( $\beta_{ND}$ ), **Heavy** ( $\beta_H$ ) or **Mostly** ( $\beta_M$ ) traffic imbalance classes of ASes.*

A default parameter setting is considered in this paper:

- **Balanced ; Not Disclosed** :  $\beta_B = 0$
- **Mostly** :  $\beta_M = 0.75$
- **Heavy** :  $\beta_H = 0.95$

An edge  $e_{i \leftrightarrow j}$  is thus decomposed in two directed edges  $e_{i \rightarrow j}$  and  $e_{i \leftarrow j}$  of different weight. If  $\beta_B = 0$ , Eq. (1) or Eq. (2) are equivalent, and each directed edge is being assigned the full `port_size` in weight. With the default setting, a heavy (resp. mostly) outbound AS is connected to its neighbors with outgoing edges of weight equal to the full port size, and with incoming edges of weight equal to 5% (resp. 25%) of the port size.

Our model captures capacities of provisioned links in the Internet, which is of course different from the traffic exchanges occurring in reality. It corresponds to an upper limit of real traffic. In the following, we use this loose upper-bounded definition of traffic to describe the provisioned bandwidth of Internet players. Thus, every time we use the term ‘traffic’ we refer to the oriented link capacities of  $W$ .

### 3.2 Parameters and network stability

Parameters  $\beta_H$  and  $\beta_M$  control the capacity imbalance between outbound and inbound edges. The *pDB c-graph* would benefit from a non-uniform personalized  $\beta$  to capture real world traffic imbalance but such data is rarely disclosed. We keep thus a uniform value of  $\beta_H$  and  $\beta_M$ , and question here their influence on the network topology. To do so, we generate 400 networks for 20 equally-spaced

values of  $\beta_H \in [0.9, \dots, 1]$  and of  $\beta_M \in [0.6, \dots, 0.8]$ . To measure the impact of these parameters, we select for each `info_ratio` category the 4 ASes that rank best in `port_capacity`, and for these ASes, we record their centrality in the network with PageRank (PR) [15] and reverse PageRank (rPR) [16]. PageRank is a measure of nodes importance in terms of the weighted incoming links, in our case the ability of a node to capture traffic from the rest of the network. The ability of a node to disseminate traffic is also of interest and is obtained by computing PageRank on the same graph but with all links inverted. This centrality is known as reverse PageRank.

We observe that  $\beta_H = 1$  causes a disruption since HO ASes like Facebook or Netflix have no incoming traffic, resulting in ranking them last in PageRank. This situation being not realistic, we exclude the corresponding networks from the results of Table 2. This table lists PR and rPR values of the 16 ASes when the network is constructed with default parameters ( $\beta_H = 0.95, \beta_M = 0.75$ ), and most importantly, the maximum variation of these values over the  $\sim 400$  graphs. The lower these variations, the less sensitive PR and rPR centrality metrics are to the choice of  $\beta_H$  and  $\beta_M$ .

First, balanced ASes are very stable in rPR and PR as expected. Our results show that outbound ASes are stable with respect to rPR and inbound ASes are stable with respect to PR. For these ASes, the default parameters create a representative network. Conversely, outbound ASes have a high  $\Delta$ rPR and inbound ASes a high  $\Delta$ PR. This last observation shows that we can only analyze outbound ASes with rPR metric and inbound ASes with PR metric to keep results calculated with the default parameter set representative. Thus, in the rest of the paper, *pDB c-graph* is constructed with default parameters, and all investigations related to outbound (resp. inbound) ASes are made with rPR (resp. PR) metric.

### 3.3 Traffic balance at IXPs

In order to verify the consistency of PeeringDB data, we study for each IXP the traffic imbalance induced by the `port_size` of its participants. By definition, traffic at IXPs is balanced between inbound and outbound flows. Since our graph model builds on the `port_size` and `info_ratio` reported by ASes, exhibiting balanced traffic at IXPs asserts the consistency of PeeringDB data and shows that our graph holds as a reasonable model of Internet peering.

The `port_capacity` metric is directly related to our *pDB c-graph* definition as follows. Let  $w_{\text{in}}^i = \sum_j W_{ij}$  be the weighted incoming degree and  $w_{\text{out}}^i = \sum_j W_{ji}$  the weighted outgoing degree. For an inbound AS  $i$ , it is clear from (1) that

$$w_{\text{in}}^i = \text{port\_capacity}(i), w_{\text{out}}^i = (1 - \beta) \cdot \text{port\_capacity}(i).$$

In the same way, for  $i$  outbound,

$$w_{\text{in}}^i = (1 - \beta) \cdot \text{port\_capacity}(i), w_{\text{out}}^i = \text{port\_capacity}(i).$$

Table 2: AS rank stability to model parameters. *PageRank (PR)* and *reverse PageRank (rPR)* values correspond to  $(\beta_H = 0.95, \beta_M = 0.75)$ .  $\Delta PR$  and  $\Delta rPR$  correspond to the variation of PR and rPR observed for the  $19 \times 20$  graphs created with  $(\beta_H, \beta_M) \in [0.9, \dots, .1] \times [0.6, \dots, 0.8]$ . IR column represents the `info_ratio` label following the notation of Table 1. We use the 2020-01-01 snapshot with *pDB c-graph* of size  $N = 10381$ .

	IR	PR	$\Delta PR$	rPR	$\Delta rPR$
Facebook	HO	124	1015	4	0
Akamai	HO	172	1330	7	1
StackPath (Highwinds)	HO	314	2214	16	2
Netflix	HO	255	1853	11	0
Apple	MO	34	29	9	0
Google	MO	27	17	8	1
Microsoft	MO	41	32	10	0
Cloudflare	MO	56	33	12	2
Amazon.com	B	4	0	5	1
Hurricane Electric	B	7	2	19	2
Core-Backbone	B	70	4	96	2
Telefónica Germany	B	72	8	100	4
KPN-Netco	MI	32	5	150	58
SoftBank Corp.	MI	69	3	272	131
Vodafone Germany	MI	86	14	360	176
Saudi Telecom Company	MI	104	12	390	176
Telekomunikasi Indonesia	HI	153	18	2041	5412
Charter Communications	HI	175	11	2233	5431
Open X Tecnologia	HI	103	15	1539	5149
OPTAGE	HI	334	15	3230	5669

But these relations do not hold for IXPs since `port_capacity` is induced by the membership of ASes. Therefore, we can assert the correctness of AS reported `info_ratio` and by extension the consistency of our model in studying the normalized traffic balance at IXPs given by  $B(i) = (w_{\text{out}}^i - w_{\text{in}}^i) / (w_{\text{out}}^i + w_{\text{in}}^i)$ . This balance ranges from -1 to 1, with 0 representing a balanced IXP. We show in Figure 2 that IXPs are overall balanced with a mean  $\langle B \rangle = 0.00 \pm 0.26$  and respective quartiles (Q1, Q2, Q3) at (-0.12, 0.00, 0.10). These results show that, at the local scale of IXPs, PeeringDB data gives a consistent view of AS membership, port size and `info_ratio` metadata.

## 4 Leveraging complex Internet network analysis

The goal of this section is to gain insight into the peering ecosystem solely from the *pDB c-graph* structure. We first present a general overview of the graph



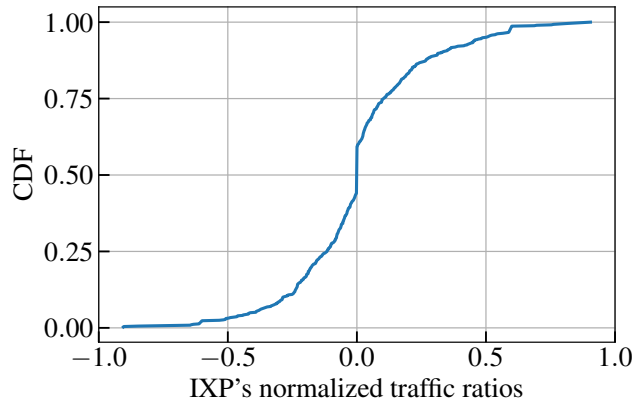


Figure 2: IXPs normalized traffic ratios or balance  $B$ .

that underlines the complex network nature of PeeringDB, reporting on topology metrics such as degree and weight distributions, and the relationship between `port_capacity` and node degree of ASes. Motivated by the fact that most of today’s Internet traffic flows from hypergiants to regional eyeball networks, we show in a second part how to recover these key peering actors in an unsupervised manner.

## 4.1 Overall graph description

As of 2020/01/01, it consists of 9695 ASes that are linked to 686 IXPs by 52422 links. Over 99% of all nodes belong to the largest connected component of the graph

### 4.1.1 Impact of weighting the edges

First of all we illustrate the benefits of weighting the bipartite graph with directional `port_size` by comparing the PR and rPR centralities of our model to the ones obtained with the non-weighted non-oriented IXP graph of Nomikos et al. [10]. For the *pDB c-graph*, differentiating the `port_size` on the oriented edges offers a clear distinction between the role of nodes. A node with high PR (rPR) is likely to receive (send) a large amount of traffic. Results for PR and rPR are shown in Table 3: top-15 PR nodes are essentially IXPs that represent the authorities in our *pDB c-graph*, while top-15 rPR identify hypergiants that diffuse their content in the network. Such a clear distinction is not present in a network model where edges are neither weighted nor oriented. For instance, an undirected graph can’t distinguish the strong diffusion of content providers like Facebook, Amazon, Netflix or Akamai from the central role of large IXPs.

Table 3: Comparison of the top 15 PageRank and reverse PageRank of IXP/AS network using our *pDB c-graph*, and the model of [10]. *Graphs are constructed for 2020-01-01 ; ASes are highlighted in bold font.*

	PageRank <i>pDB c-graph</i>	PageRank graph of [10]	Reverse PageRank <i>pDB c-graph</i>
1	IX.br São Paulo	IX.br São Paulo	IX.br São Paulo
2	DE-CIX Frankfurt	AMS-IX	DE-CIX Frankfurt
3	AMS-IX	DE-CIX Frankfurt	AMS-IX
4	<b>Amazon</b>	LINX LON1	<b>Facebook</b>
5	LINX LON1	EPIX.Katowice	<b>Amazon</b>
6	NAPAfrica IX J.	Mumbai IX	LINX LON1
7	<b>Hurricane Electric</b>	NAPAfrica IX J.	<b>Akamai</b>
8	Equinix Singapore	France-IX Paris	<b>Google</b>
9	NL-ix	SIX Seattle	<b>Apple</b>
10	SIX Seattle	NL-ix	<b>Microsoft</b>
11	Equinix Ashburn	IX.br Rio de Janeiro	<b>Netflix</b>
12	EPIX.Katowice	TorIX	<b>Cloudflare</b>
13	IX.br Rio de Janeiro	EPIX.Warszawa-KIX	NL-ix
14	Equinix Chicago	LINX LON2	Equinix Singapore
15	Netnod Stockholm	Equinix Ashburn	NAPAfrica IX J.

#### 4.1.2 Degree and port\_capacity distributions

Probability distributions of undirected nodes degree  $d$  and port capacity for the *pDB c-graph* are shown in Figure 3. From our model definition, this degree is equal to the degree of incoming links and to the degree of outgoing links.

The probability distribution of node degree is generally well approximated by a power-law, a feature commonly found in other real networks [19]. Power-law exponent of ASes degree distribution  $\gamma = 2.69$  falls in the range [2, 3] usually reported for real networks [20] and shows that the repartition of ASes degree is heterogeneous, especially compared to the IXPs, whose degree distribution is fitted with  $\gamma = 1.53$ . `port_capacity` distribution follows a heavy-tailed distribution found in other weighted networks such as the world-wide airport traffic network [21], where authors introduce a “node strength” metric analogous to our `port_capacity`.

As opposed to the latter network of [21], we do not find in Figure 4 a particularly linear relation between AS degree and `port_capacity`. We attribute this observation to the fact that port size may vary from several orders of magnitude (100M to 1T), while airplanes carry tens to hundreds of passengers. Interestingly, we find outliers that present different peering strategies. Regional Network Service Provider KPN-Netco ranks 15 in `port_capacity` with only  $d = 3$ . On the other hand, ASes that support public Internet services (e.g. DNS) such as both Packet Clearing House (PCH) ASes and VeriSign Global Registry Services respectively rank according to the degree 3rd and 4th for PCH, and 13th for VeriSign, with a `port_capacity` of about two orders of magnitude lower than the hypergiants that exhibit similar values of degree.

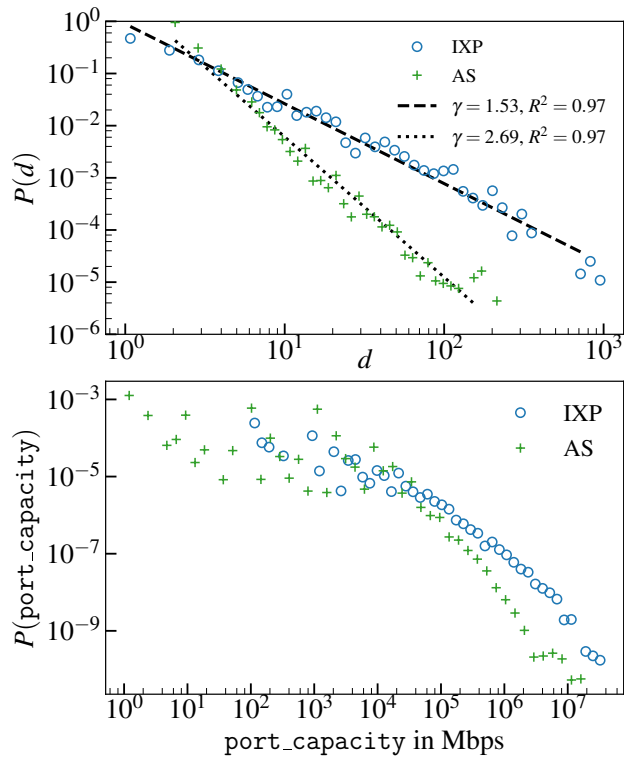


Figure 3: *pDB c-graph* degree and weight distributions. Degree distributions follow a power-law  $f(x) = Ax^{-\gamma}$ .

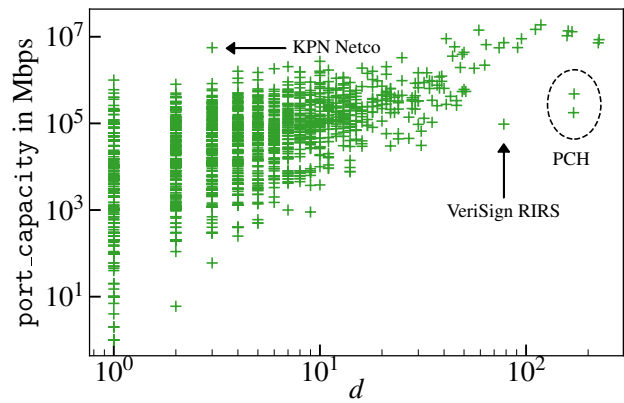


Figure 4: `port_capacity` versus node degree  $d$  for ASes.

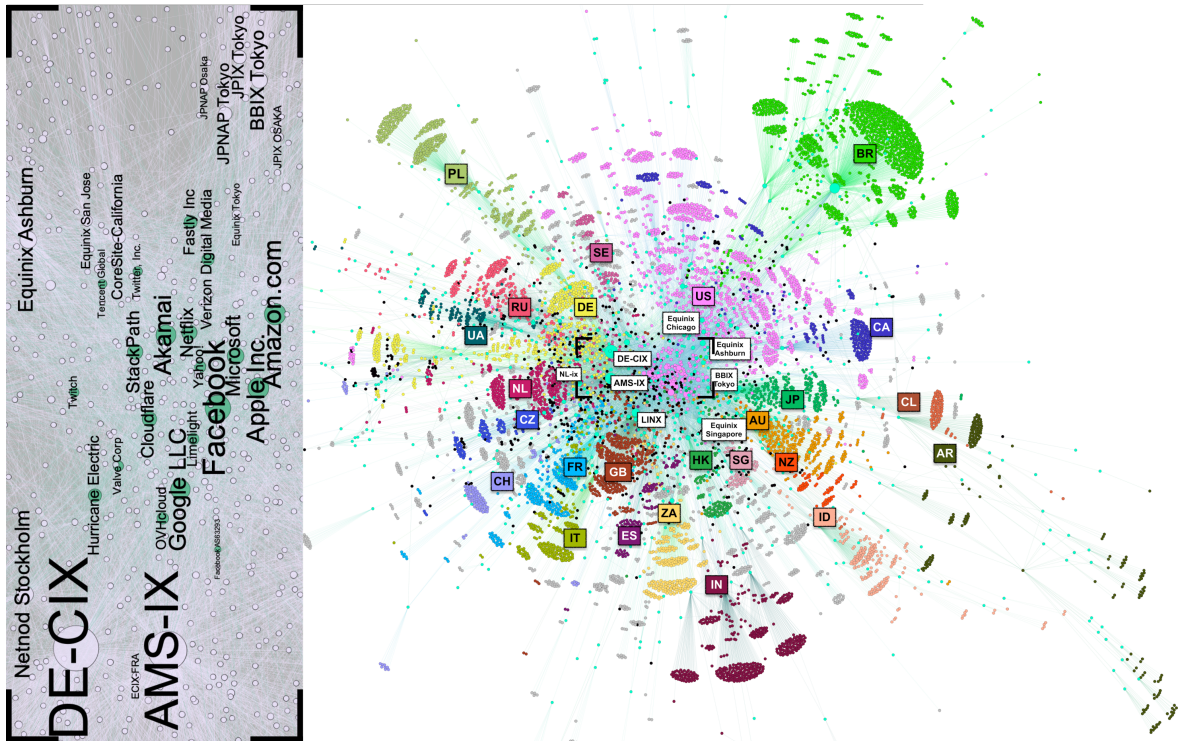


Figure 5: *pDB c-graph*: Visualization of ASes classified by countries plot using OpenOrd and Yifan Hu layouts of Gephi [17]). *Node size is proportional to port\_capacity and cluster colors are indicated with country label colors for a selection of the largest 25 clusters. IXP node color is light blue and ASes identified as tied are black. On the left, an inset figure zooms on the position of the 20 hypergiant content providers, together with the largest IXPs, located at the center of the graph. Graph can be navigated interactively at [18].*

## 4.2 Retrieving key peering actors

We now investigate the structural properties of the graph in order to retrieve the main peering actors. We first start by deriving a country classification of ASes and proposing a visualization of the graph. We identify hypergiants with the reverse PageRank network metric, and show with the visualisation their global reach. Then for countries of interest we extract the main traffic receivers with PageRank metric, and show that identified ASes relate to eyeball networks.

### 4.2.1 *pDB c-graph* regional structure

We aim at refining the geographical information reported by ASes in PeeringDB under the label `info_scope`. This attribute can either be referenced with the name of a continent or as `Global`, `Regional`, `Not Disclosed`. Refining allows to

Table 4: ASes country classification metrics. *Ground-truth data is obtained from [22], and prediction is based on the country of the majority of IXPs an AS belongs to.*

Country	Precision	Recall	F1-Score	Support
US	0.88	0.89	0.88	1360
CA	0.93	0.80	0.86	297
BR	0.99	0.99	0.99	1302
DE	0.75	0.86	0.80	484
NL	0.73	0.81	0.77	288
GB	0.90	0.76	0.82	440
FR	0.92	0.86	0.89	308
IT	0.94	0.91	0.93	228
ES	0.96	0.90	0.93	114
RU	0.90	0.91	0.90	290
PL	0.98	0.96	0.97	421
CN	0.79	0.48	0.60	56
IN	0.99	0.98	0.99	438
JP	0.92	0.96	0.94	227

narrow down ASes location from continent-level to country-level, which is particularly needed since 45% of ASes are reported as `Regional` or `Not Disclosed`. In order to attribute countries to ASes, we refer to their relationships with IXPs. Indeed, IXPs have accurate `country` labels. Therefore, we assign to an AS the country of the majority of IXPs it belongs to. For 5.46% of ASes there is no majority, and we give them the label `Tied`.

The geographical classification has been assessed by Caida AS organizations dataset [22]. This dataset maps ASes to organizations, and retrieve organizations' country with regional Internet registries WHOIS entry or by inference. By considering this dataset as ground-truth, classification metrics such as precision, recall and F1-score are computed and presented in Table 4. Recall is defined as the ratio of the true positives to the union of true positives and false negatives and precision is the ratio of the true positives to the union of true positives and false positives. High recall minimizes false negatives while high precision minimizes false positives. Finally, F1 score is an harmonic mean of precision and recall. High F1 score occurs if both recall and precision are high. We confirm that overall, country classification based on ASes' proximity to IXPs in PeeringDB is in good accordance with Caida.

We question if this geographical classification is consistent with the structure of the *pDB c-graph*. To answer this question, we propose a visualization of the *pDB c-graph* of 2020-01-01 in Figure 5. The graph layout, computed with the automatic Yifan Hu force-directed algorithm of Gephi [17], is available to be interactively navigated in [18]. The geographical distribution of ASes is in good accordance with the *pDB c-graph* structure. Links and their weights

Table 5: Hypergiant ASes: Top 20 ASes in reverse PR in *pDB c-graph* of 2020-01-01. *ASes identified as hypergiants in [2] are listed in bold font.*

Rank	Name	Rank	Name
1	<b>Facebook</b>	11	Fastly
2	<b>Amazon</b>	12	<b>Edgecast</b>
3	<b>Akamai</b>	13	<b>OVHcloud</b>
4	<b>Google</b>	14	<b>Limelight Networks Global</b>
5	<b>Apple</b>	15	<b>Yahoo!</b>
6	<b>Microsoft</b>	16	Valve Corporation
7	<b>Netflix</b>	17	<b>Twitch</b>
8	<b>Cloudflare</b>	18	Tencent Global
9	StackPath	19	<b>Twitter</b>
10	<b>Hurricane Electric</b>	20	CABASE-RCB

arrange the nodes such as to structure the graph around areas of influence of IXPs, which tend to be correlated with their geographical location. The ASes identified as **Tied** are spread evenly across the network and are often peering at a few IXPs of different countries. Interestingly, the graph topology not only groups ASes per countries, but keeps the geographical proximity of countries. For instance, the upper left part of the graph groups Northern and Eastern European countries, while the lower left groups Central European ones. The lower right part groups Asian and Oceanian countries, while the upper right groups the USA, Canada and Southern-American countries. This relation between regional and structural proximity is also found with Louvain method, an unsupervised clustering technique presented in Appendix Appendix B.

#### 4.2.2 IXPs and hypergiants global reach

We extract the best 20 highly diffusive ASes with reverse PageRank metrics. These ASes, listed in Table 5, encompass the 15 hypergiant ASes of [2], most of them being content providers. In the rest of this paper, we identify this set as the set of hypergiants. In Figure 5, highlighted with an inset view, we find hypergiants and important IXPs that play a central role since they have a very large number of links. For instance, content providers such as Cloudflare, Akamai, Microsoft, Facebook, Amazon or Netflix are respectively connected to 226, 160, 158, 118, 111 or 95 IXPs. Hurricane Electric, PCH or VeriSign are connected to 224, 170 or 78 IXPs. Central IXPs like DE-CIX Frankfurt and AMS-IX interconnect the hypergiants to European ASes, while Japanese connect them to Asia and Oceania. US-based Equinix IXPs link the US ASes to the rest of the network. The set of ASes connected to a single IXP is represented with an umbrella shaped form. These ASes are mostly of **Cable/DLS/ISP** type. The closer to the center an AS is, the higher its degree gets as it is connected to multiple IXPs. We observe as well that higher degree ASes are tagged with **NSP**

Table 6: ASes end-users market share by country. *The AS selection differs, from the first to the last line: all APNIC ASes, ASes present in both PeeringDB and APNIC, the top4 ASes by EUMS present in both PeeringDB and APNIC, the top 4 PR ISP and Not Disclosed ASes, traffic receivers (defined in the body).*

Selection procedure	US	CA	BR	DE	NL	GB	FR	IT	ES	RU	PL	CN	IN	JP
APNIC	96.61	99.49	94.57	99.36	99.67	99.39	99.67	99.55	99.72	98.24	99.11	99.85	99.24	99.69
PeeringDB and APNIC	32.46	86.88	53.44	92.84	86.55	87.44	57.27	60.28	56.75	40.25	37.25	56.44	9.96	92.12
PeeringDB and APNIC top4	18.78	52.98	29.75	60.38	66.01	61.85	51.75	53.95	49.52	30.09	26.64	56.07	4.34	63.54
Top4 PR ISP/ND	<b>13.67</b>	3.44	13.84	24.32	7.81	<b>43.98</b>	<b>28.09</b>	13.23	<b>45.07</b>	0.71	<b>15.82</b>	0.01	<b>3.32</b>	14.54
Traffic receivers	<b>9.57</b>	3.44	13.87	29.38	32.77	<b>42.02</b>	<b>28.04</b>	<b>50.12</b>	<b>46.38</b>	0.01	<b>19.65</b>	0.00	<b>3.33</b>	21.96

(Network Service Provider) or **Content** type in majority. This last observation, explored further in the next sections, reveals a geographic proximity that is leveraged by hypergiants to reach global and regional NSPs and ISPs through peering exchanges points.

### 4.2.3 Eyeball networks

We saw that hypergiants are easily identified with *pDB c-graph*. Now that we know from where most of the traffic originates, we question here if ASes closest to end-users, known as eyeball networks, can be retrieved from PeeringDB. Intuitively, we expect these networks to be characterized by a strong inbound behavior in their geographical area of influence. As such, we will identify them using PR metric and the geographical information of *pDB c-graph*.

For the validation, we consider the APNIC customers per AS datasets [23]. APNIC, via ad-based measurements, estimates for each eyeball ASes their end-user market share (EUMS) by country. We check first if APNIC eyeballs are covering, for 15 countries of interest, 100% of the population. We see in Table 6, APNIC ASes entry, that the agglomerated EUMS is generally close to 100%. However, if we select ASes that are both in APNIC and PeeringDB (cf. line 2 of table Table 6), this percentage drops more or less dramatically, depending on countries. The most underrepresented countries are India, Poland and the USA which underlines that eyeball ASes in these countries can't or don't leverage IXPs. Another limitation is that some eyeball ASes do not benefits from public peering, and therefore are not present in *pDB c-graph*. For example ISP Comcast, with 15% market share in the US, does not report membership in public peering exchanges as a consequence of a paid peering policy [24].

We expect eyeball ASes to have an inbound nature and a regional presence visible in the structure of *pDB c-graph*. To identify them, we select for each country a subset of ASes with reported business type **DSL/Cable/ISP** or **Not Disclosed**. In this subset, we retrieve the top 4 traffic receivers, i.e. ASes that rank in the top 4 according to PageRank. We exclude from this set the ASes already present in the hypergiants set. We check if these ASes are present in APNIC and retrieve their EUMS (Table 6 entry Top4 PR ISP/ND). We compare this number to the best accessible EUMS, i.e. the agglomerated EUMS of the top4 ASes present in both APNIC and PeeringDB (Table 6 entry PeeringDB and APNIC top4). For 6 countries highlighted in bold, our procedure recovers more

than half of the best accessible EUMS, showing that *pDB c-graph* can recover some regional eyeball networks. We can improve our results by considering NSPs as well as ISPs and then manually remove Not Disclosed or NSPs ASes that do not have end-user customers. We call ASes identified with this procedure “traffic receivers”. The aim is not to optimize the EUMS but rather to remove obvious wrongly identified ASes with as little alteration as possible. We have removed Verisign, Telegram Messenger, and the 4 tier-2 ISPs: Core-Backbone, Open Peering, Orange Polska and Brightwave. We observe that Canada, Russia and China eyeballs are not well recovered, mainly because of our clustering procedure miss-assigning them to the US. For other countries, we identified networks that reach a significant part of the population.

The main regional traffic receivers identified by our procedure are shown in Table 7. We see that PeeringDB derived country clustering is in good accordance with APNIC countries<sup>3</sup>. A notable mislabeling is the attribution in the US of NSP KDDI, representing 20% of Japan EUMS. Almost all ASes identified are present in APNIC. For most countries, we are able to retrieve at least one or two ASes with a high ranking in APNIC. In the next parts, we will characterize how these eyeballs capture hypergiants’ content.

## 5 Deriving AS-AS traffic exchanges to study hypergiants diffusive patterns

ASes engages peering sessions at IXPs in order to exchange traffic. To fully capture these interactions, one would have to obtain a traffic matrix for each IXP. Such traffic matrices are not publicly disclosed, and only a few of them has been described in the scientific literature over the past years [7] [8] [3]. Capturing AS to AS traffic exchanges occurring at IXPs is therefore not achievable at a global scale and within a short-time resolution of a day.

In this section, we show that the graph formulation of PeeringDB, coupled with stochastic complementation from Markov chain theory, can partially address this problem. In simple worlds, we rely on co-occurrence of ASes at IXPs, weighted by the port sizes and ASes reported ratio between inbound and outbound traffic, to approximate ASes traffic exchanges at a global scale. Our method consists in two steps i) building a Google matrix that encodes interactions of *pDB c-graph* ii) computing a reduction of this matrix, called the reduced Google matrix, for only nodes of interests. The matrix reduction allows us to censor IXPs and retrieve only indirect AS-AS interactions. We will use it to study the diffusive patterns of hypergiants toward the main regional traffic receivers identified in last section. In the rest of the paper, we refer to the *reduced network of ASes* as the union of hypergiants and regional eyeballs listed in both Table 5 and Table 7.

---

<sup>3</sup>For an AS with presence in multiple countries, we selected the country where the AS has the largest EUMS.



Table 7: Main regional traffic receivers. *ASes are retrieved with the procedure described in subsection 4.2.3.*

Name	PeeringDB		APNIC		
	CC	Rank	CC	Rank	EUMS
T-Mobile USA	US	1	US	2	9.53
Claro S.A.	US	2	BR	24	0.16
Zayo	US	3	US	44	0.04
KDDI	US	4	JP	1	19.76
Open X Tecnologia	BR	1	BR	40	0.0
G8	BR	2	BR	35	0.05
Claro S.A. (NET)	BR	3	BR	1	13.82
Sistemax Brasil	BR	4	BR	40	0.0
Telefónica DE	DE	1	DE	3	10.14
Vodafone DE	DE	2	DE	2	11.61
Saudi Telecom Company	DE	3	SA	17	0.0
Vodafone Kabel DE	DE	4	DE	5	7.63
KPN-Netco	NL	1	NL	1	29.85
BICS	NL	2	CN	39	0.0
T-Mobile Thuis	NL	3	NL	6	2.92
Joint Transit	NL	4			
BTnet	GB	1	GB	3	16.77
TalkTalk	GB	2	GB	5	5.77
Sky Broadband	GB	3	GB	1	19.21
Hyperoptic	GB	4	GB	20	0.27
Bouygues Telecom ISP	FR	1	FR	4	13.65
SFR Group	FR	2	FR	3	14.37
Zayo France	FR	3	FR	21	0.02
moji	FR	4	FR	23	0.0
WIND Telecom.	IT	1	IT	3	17.02
NGI	IT	2	IT	8	1.37
Fastweb	IT	3	IT	4	10.44
Vodafone Italy	IT	4	IT	2	21.29
MásMóvil	ES	1	ES	4	6.35
Orange Spain	ES	2	ES	2	24.92
Vodafone España	ES	3	ES	3	13.63
Aire Networks del M.	ES	4	ES	10	1.48
Netia S.A.	PL	1	PL	5	3.92
VECTRA	PL	2	PL	6	3.38
Polkomtel	PL	3	PL	2	12.27
Korbank	PL	4	PL	26	0.08
SoftBank	JP	1	JP	2	19.23
Level 3 AS 3356	JP	2	US	39	0.09
Colt	JP	3	DE	30	0.09
BIGLOBE	JP	4	JP	8	2.73

## 5.1 Node censoring and graph reduction

### 5.1.1 Google matrix

From the weighted oriented matrix of a network of size  $N$ , the Google matrix  $G$  is a stochastic matrix defined by  $G_{ij} = \alpha S_{ij} + (1 - \alpha)/N$  with  $S$  the Markov transition matrix whose elements follow:

$$S_{ij} = \begin{cases} W_{ij}/w_{\text{out}}^j & \text{if } w_{\text{out}}^j > 0, \\ 1/N & \text{otherwise.} \end{cases}$$

The damping parameter  $0 \leq \alpha < 1$  insures the irreducibility of  $G$ , that is for any normalized vector  $P$  the iterative product  $P = GP$  converges to a stationary distribution called the PageRank vector. Standard value for  $\alpha$  is 0.85 as given in the state-of-the-art work of Brin and Page [15].  $P(i)$  is the probability of finding a random surfer at node  $i$  if we let him surf the graph for an infinitely long time following the Markov transition probabilities of  $G$ . Thus sorting  $P$  by descending values ranks the nodes from the most influential nodes in terms of incoming links to the less influential node. This ranking is called the PageRank centrality PR. Reverse PageRank is calculated by simply transposing  $W$ , which resumes to inverting all the links in the graph.

### 5.1.2 Reduced Google matrix

The reduced Google matrix describes the properties and interactions of a given subset of nodes belonging to a much larger directed network [25]. It is derived using a dedicated algorithm which is based on the stochastic complementation [11] of the Google matrix.

For a subset of  $N_r$  nodes of interest selected in  $\mathcal{G}$ , we can define a reduced network by reordering rows and columns of  $G$  in the following block structure:

$$\tilde{G} = \begin{bmatrix} G_{rr} & G_{rs} \\ G_{sr} & G_{ss} \end{bmatrix}$$

where the index  $r$  refers to the nodes of the reduced network and  $s$  to the nodes in the complementary network. By noting the Pagerank vector as  $[P_r, P_s]^T$  that satisfies  $\tilde{G}P = P$ , we define the *reduced Google matrix*, noted  $G_R$ , as  $G_R P_r = P_r$ . From the block structure of  $\tilde{G}$ ,  $G_R$  can also be defined as the Schur complement of the block  $G_{ss}$  with:

$$G_R = G_{rr} + G_{rs}(\mathbf{1} - G_{ss})^{-1}G_{sr}. \quad (3)$$

The matrix  $G_R$  represents an equivalent Markov chain whose transition probabilities capture the interactions between the subset of selected nodes by direct and all possible indirect (multi-hop) links present in the network of origin.

## 5.2 Hypergiants diffusive patterns

To study hypergiants diffusive patterns, we construct a reduced Google matrix encompassing them and the main regional traffic receivers. The benefits of the reduction are two-fold. First, by censoring the IXPs, we obtain AS-AS interactions. Second, by censoring all the other ASes, we obtain a smaller and intelligible Google matrix.

We saw that PageRank is a measure of centrality in terms of incoming links. In *pDB c-graph*, the PageRank centrality naturally captures the capacity of nodes to concentrate traffic. In order to study the nodes capacity to send traffic and its diffusive patterns, we make use of the reverse PageRank metric by calculating the stochastic complement of the inverted *pDB c-graph*. We note  $G^*$  and  $G_R^*$  the Google matrices associated to such a graph. In this case, the  $(i, j)$  element of  $G_R^*$  represents the probability, through direct and indirect links, that traffic arriving to node  $j$  originates from  $i$ . For the analysis, we don't show the diagonal values that represents self-loop traffic of an AS which is not of interest in this paper. To do so, we have to set diagonal value to 0 and re-normalize column-wise to get a stochastic matrix.

The matrix of direct and indirect interactions  $G_R^*$ , represented in Figure 6, shows two interesting properties. The first one is the block of strong links in the top right corner, identified with white dotted lines, that depicts the hypergiants diffusion to main regional ISPs. The concentration of links in this area confirms the grasp of hypergiants on regional ISPs. The second property is the block structures appearing on the matrix diagonal, highlighting local traffic exchanges enabled by IXPs. In particular, we report a strong link in the Netherlands between KPN-Netco and Joint-Transit, resulting from the fact that both players have their large port sizes solely at the same IXPs NL-ix and NL-ix2. This link captures the possible capacity that is offered by the physical network peering infrastructure to interconnect both ASes. However, there is currently is no AS path that reports both ASes in the BGP control plane. We can conclude this link shows that they benefit from interactions with the same third-party ASes in this case.

## 6 Use case on COVID-19 demand for content

In the previous sections, we saw that *i*) hypergiants are at the core of the *pDB c-graph* and have a global reach and that *ii*) the *pDB c-graph* structure reveals geographic proximity between hypergiants and regional eyeball ISPs.

Hypergiant content delivery networks (CDN) connect to regional ISPs at IXPs to improve end-user experience [26] and widen their reach. Covid-19 outbreak lead to a larger capacity demand from end-users [27] [28], forcing hypergiants to adjust their peering strategy by increasing total port size between 2019-01-01 and 2021-03-01 as seen in the PeeringDB global port capacity evolution of Figure 1. However it is not clear yet to what extent their proximity with regional ISPs has changed. In this last part, we aim at identifying how

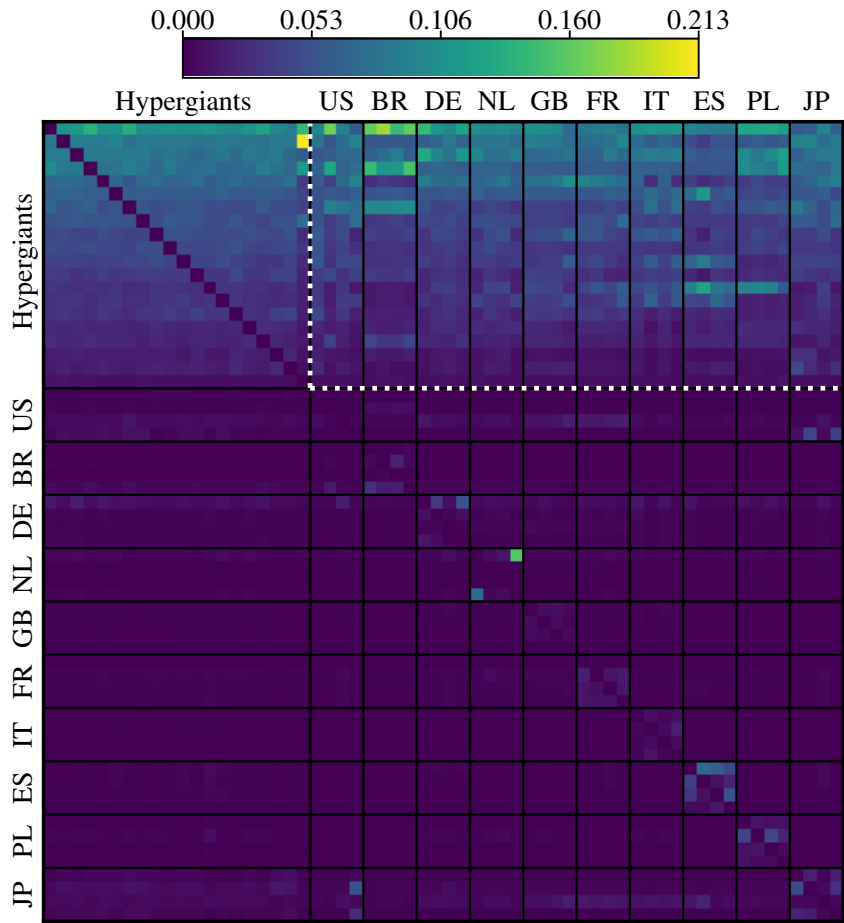


Figure 6: Reduced Google matrix  $G_R^*$  for the reduced network of hypergiants and traffic receivers. *Hypergiants* (resp. *traffic receivers*) are listed in the order of Table 5 (resp. Table 7). The block encased in white dotted lines represents the hypergiant to traffic receivers diffusion part.

hypergiants have increased or decreased their reach towards eyeballs using a reduced Google matrix analysis.

Therefore, we derive first the Google matrix of the full *pDB c-graph*. Next, we compute the Google matrix  $G_R^*$  of the reduced network of ASes, this matrix encoding hypergiants diffusion to eyeballs. We compute  $G_R^*|_{d1}^{d2}$ , the relative change of the elements of  $G_R^*$  between two dates  $d1$  and  $d2$  given by

$$G_R^*|_{d1}^{d2}(i, j) = \frac{G_R^*|_{d2}(i, j) - G_R^*|_{d1}(i, j)}{G_R^*|_{d1}(i, j)}. \quad (4)$$

Results are shown in Figure 7. For better visibility we limit the colormap to the interval ranging from -0.5 to 1.0, where -0.5 represents a 50% decrease of a link from its initial value and 1.0 a 100% increase. For the first period, the capped links are Netflix  $\rightarrow$  Zayo France, Netflix  $\rightarrow$  WIND Telecom with respective values 1.07, 1.03. For the second period, the capped links are Cloudflare  $\rightarrow$  Zayo France, Cloudflare  $\rightarrow$  G8 with values 1.34 and 1.09.

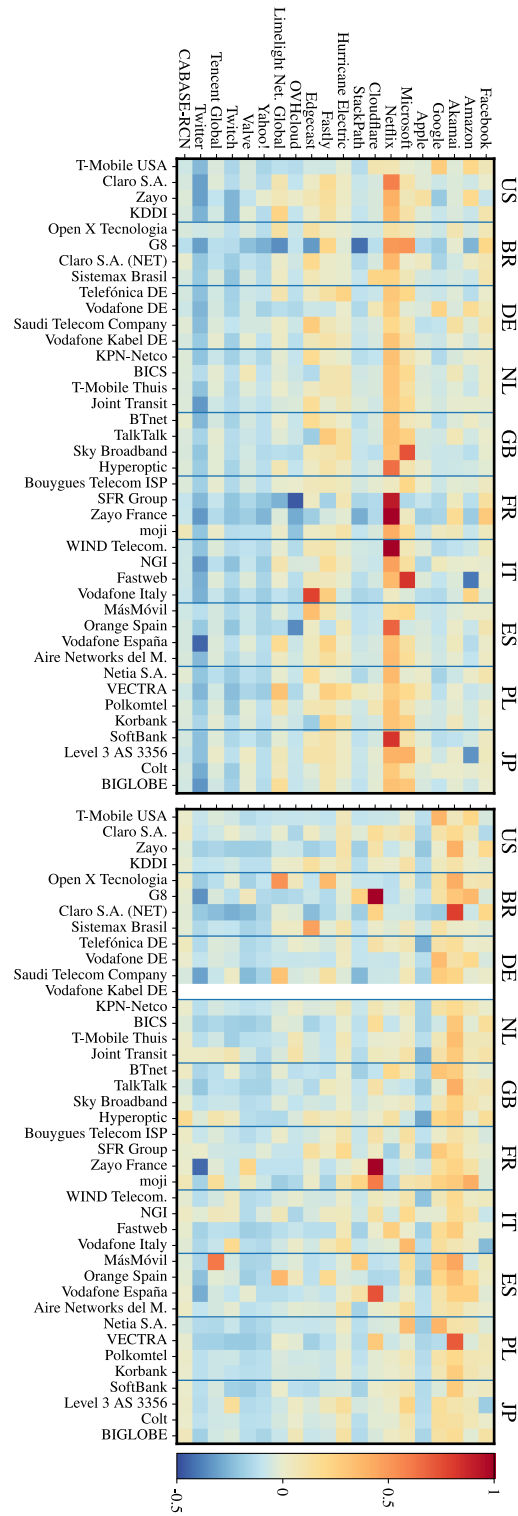


Figure 7: Relative time change of reduced Google matrices  $G_R^*_{2020-06-01}^{2021-01-01}$  (left panel) and  $G_R^*_{2020-06-01}^{2020-06-01}$  (right panel). Only the top right part of  $G_R^*$  is shown, corresponding to the hypergiants diffusion to traffic receivers part.

During Covid outbreak, the biggest links increase are found for Netflix → (WIND Telecom, Zayo France, SFR Group, SoftBank), Microsoft → (Fastweb, Sky Broadband) and Edgecast → Vodafone Italy. The negative changes are OVHcloud → (SFR group, Orange Spain), Twitter → Vodafone España, Stack-Path → G8. We compute the sum of each line to determine which ASes have invested the most. Netflix is ahead by far, investing mainly in France, Italy, Japan and Great Britain, followed by Microsoft that invested in Great Britain, Italy and Japan, and then by Fastly in Poland, Italy, Great Britain, and finally Edgecast in Italy and Spain. Netflix indeed reports an increase in capacity at IXPs to face a growing end-user demand during the outbreak [5]. ASes that invested the least are Twitter, Twitch, Yahoo! and OVHcloud.

Post-outbreak, the biggest links increase are found for Cloudflare → (Zayo France, G8, Vodafone España) and Akamai → (Claro SA, Vectra). The negative changes are notably Twitter → (Zayo France, G8, Saudi Telecom Company) and Apple → Hyperoptic. The top investors are Akamai in Brazil, Poland, Great Britain, Spain and the Netherlands, followed by Google in Germany, Spain and France, and then Cloudflare in France and Brazil. ASes that invested the least are Twitter, Apple, Yahoo! and Valve.

## 7 Related works

**IXP for Internet topology** Internet topology being extensively measured and modeled over the last years, we restrict ourselves to the role IXPs played in the Internet topology. For an overview of AS-level studies, we refer the reader to [29] and to the related works section of [10].

Previous work of Ager et al. [3] shows that a single large European IXP presents more peering links than inferred for the Internet-wide AS-level topologies based on traceroute and BGP data. Access to the IXP traffic matrix and participants metadata allows the authors to characterize the diversity of the Internet ecosystem, revoking the classical AS tier classification. The global role of the same IXP is identified in [26], where authors argue that IXPs provide a good visibility of the Internet. [30] study the temporal evolution of an European IXP that gives insights on peering matrices, traffic growth, traffic imbalance and port utilization.

However, to the best of our knowledge, only a few studies have focused on the Internet-wide topology derived from public IXP datasets. An unweighted and undirected bipartite graph based on IXPs and their AS membership using data from PeeringDB [31] and Packet Clearing House [32] is proposed in [10]. This allows a first study of ASes connectivity but do not contain information on traffic flows.

**PeeringDB** A first study of PeeringDB is presented in [13]. They show that PeeringDB entries are generally up-to-date and correct, and contain precious metadata on IXPs and their participants. They point out several biases, notably regarding AS business type diversities and their geographic distribution, but

argue that PeeringDB gives a reasonable view of the peering ecosystem. A more recent overview of the dataset is presented in [2], where authors agglomerate AS port size at IXPs to introduce the `port_capacity` metric we leverage as well in this paper. Doing so, they successfully identify the hypergiants of the peering ecosystem. By combining this port size information to the bipartite model of [10], and introducing the direction of edges based on traffic imbalance metadata, we provide a weighted and directed graph that gives a coarse view of the traffic flows between the main protagonists of the peering ecosystem.

**Google matrix** PageRank [15] derived from the Google Matrix efficiently identifies popular pages of the hypertext-directed Web Graph. It has been applied to many other types of graphs [33]. In particular, combining PageRank and reverse PageRank study to the international trade network [34] allows to add new insights on money flows to the classical economic balance metric. Using this approach on our network, we are able to identify content hypergiants and main ISPs at the country level.

Stochastic complementation was proposed in [11] to build a stochastic matrix for a small subset of nodes in a large network. This reduced stochastic matrix encodes information on the subset nodes interactions between themselves and over the whole network, leading to the differentiation of direct and indirect links. In our work we use this decomposition to obtain interactions between ASes, even though they do not share direct links. By doing so, we quantify the reach of hypergiants on the main regional ISPs and show the reaction of global content providers to the pandemic.

## 8 Conclusion

This paper proposes a novel Internet network model from PeeringDB database records, *pDB c-graph*, that offers a coarse but realistic picture of the overall capacity provisioned by ASes in the peering ecosystem. Its originality lies in the weighted and oriented edges which capture the port sizes and ASes `info_ratio` labels, respectively. From this model, we are able to identify key Internet players such as the state-of-the-art hypergiants and important regional eyeball networks present in the PeeringDB database. We show that it is possible, with a stochastic matrix representation of this graph, and its stochastic complementation for a reduced set of ASes, to extract quickly their capacity of interconnection offered the global physical public peering infrastructure. As a use-case, we propose a study that quantifies and identifies the links affected by the 2020 Covid-19 outbreak as captured by the PeeringDB ASes and IXPs evolution over time. Future works will investigate multi-layer networks [35] or time-series similarity measures [36] to better model the kinetic of the *pDB c-graph*.



Table 8: IXP statistics for the 12 largest Louvain clusters of *pDB c-graph* of 2020-01-01.

Louvain Cluster	IXPs country distribution	#Different IXP countries	Grouping interpretation	Port capacity (%)	# of IXP (%)
0	US: 74 — CA: 12 — CO: 2 — GU: 2 — SG: 2	13	North America	18.5	14.6
1	DE: 22 — AT: 4 — CH: 4 — US: 2 — AE: 1	16	Germanic countries	11.7	6.4
2	FR: 15 — GB: 11 — IE: 4 — US: 3 — AU: 2	16	Western Europe	10.1	6.9
4	NL: 9 — BE: 1 — BJ: 1 — CA: 1 — IS: 1	6	Netherlands	10.1	2.0
7	BR: 34 — RO: 4 — AO: 2 — KE: 2 — US: 2	11	Brazil	8.6	7.3
8	AR: 22 — JP: 13 — CL: 6 — HK: 2 — BH: 1	10	South America, East Asia	8.3	7.1
5	ID: 16 — TH: 7 — PH: 4 — HK: 3 — SG: 3	12	South-East Asia	7.1	6.3
10	RU: 30 — UA: 12 — BG: 6 — KZ: 3 — KG: 2	12	Eastern Europe	5.9	9.0
3	SE: 10 — NO: 7 — ES: 6 — FI: 4 — DK: 3	15	Scandinavian countries	5.0	6.7
9	AU: 21 — NZ: 6 — US: 4 — MY: 1	4	Oceania Pacific	3.4	4.7
6	TZ: 5 — ZA: 5 — US: 4 — CA: 2 — CD: 2	36	Africa	2.8	7.3
14	PL: 11 — RO: 2 — PH: 1	3	Eastern Europe	2.3	2.0

## A Reproducibility of our research

We assess in this section the possibility of recreating our research. Based on ACM definitions <sup>4</sup>, a work can either be repeatable (authors can reliably repeat their own computation), reproducible (an independent group can obtain the same results using the author’s own artifacts) and replicable (an independent group can obtain the same results using artifacts which they develop completely independently).

### A.1 Repeatability

Our results are repeatable. The dumps of PeeringDB are not subject to change and the processing is deterministic.

### A.2 Reproducibility

We will make available the generated datasets of *pDB c-graph* in [12], and plan to publicly share the source codes used for the dataset generation and analysis. The *pDB c-graph* is solely constructed from the public datasets of CAIDA. Our source codes rely on commonly used Python libraries, and our C++ implementation of stochastic complementation [37] is cross-platform and self-contained thanks to CMake software development tool. We hope that these efforts will allow other researchers to reproduce and extend our results.

### A.3 Replicability

The data we provide is either directly obtained from PeeringDB or from processing. We explicitly mention in this work the data acquired from processing and did our best to provide enough information to replicate this processing. We expect other researchers to be able to replicate our implementation or data analysis since it was performed with well-documented tools.

<sup>4</sup>(<https://www.acm.org/publications/policies/artifact-review-and-badging-current>)

## B Modularity clustering

The Louvain method [38] is a simple, unsupervised and easy-to-implement method for identifying communities in large networks. Moreover, it is known to be one of the most accurate community detection algorithms [39]. This algorithm relies on a greedy optimization method that minimizes the modularity metric of partitions of the network. The modularity measure for a bipartite network was introduced in [40], and a Louvain implementation using this modularity is proposed in [41]. Since the bipartite modularity is defined for undirected networks, we apply Louvain to the undirected *pDB c-graph* of weighted adjacency matrix  $A = W + W^T$ . A link of this network corresponds to the port size an AS possesses at an IXP.

Louvain method is known to fail in detecting small communities, but we are interested in identifying larger ones. Studying the distribution of IXPs country in Louvain clusters, we observe that the algorithm grouped countries with strong relations or geographical proximity, as underlined in Table 8. Clusters grouping Northern American, Brazilian, Asian-Pacific, Scandinavian or Eastern European IXPS are observed consistently throughout our testings.

## References

- [1] E. Gregori, A. Improta, L. Lenzini, and C. Orsini, “The impact of ixps on the as-level topology structure of the internet,” *Computer Communications*, vol. 34, no. 1, pp. 68 – 82, 2011. [Online]. Available: <http://www.sciencedirect.com/science/article/pii/S014036641000383X>
- [2] T. Böttger, F. Cuadrado, and S. Uhlig, “Looking for hypergiants in peeringdb,” *SIGCOMM Comput. Commun. Rev.*, vol. 48, no. 3, p. 13–19, Sep. 2018. [Online]. Available: <https://doi.org/10.1145/3276799.3276801>
- [3] B. Ager, N. Chatzis, A. Feldmann, N. Sarrar, S. Uhlig, and W. Willinger, “Anatomy of a large european ixp,” in *Proceedings of the ACM SIGCOMM 2012 Conference on Applications, Technologies, Architectures, and Protocols for Computer Communication*, ser. SIGCOMM ’12. New York, NY, USA: Association for Computing Machinery, 2012, p. 163–174. [Online]. Available: <https://doi.org/10.1145/2342356.2342393>
- [4] N. Chatzis, G. Smaragdakis, A. Feldmann, and W. Willinger, “There is more to ixps than meets the eye,” *SIGCOMM Comput. Commun. Rev.*, vol. 43, no. 5, p. 19–28, Nov. 2013. [Online]. Available: <https://doi.org/10.1145/2541468.2541473>
- [5] G. Haspilaire. (2020) A cooperative approach to content delivery. [Online]. Available: <https://openconnect.netflix.com/Open-Connect-Briefing-Paper.pdf>
- [6] A. Feldmann, O. Gasser, F. Lichtblau, E. Pujol, I. Poese, C. Dietzel, D. Wagner, M. Wichtlhuber, J. Tapiador, N. Vallina-Rodriguez, O. Hohlfeld, and G. Smaragdakis, “A year in lockdown: How the waves of covid-19 impact internet traffic,” *Commun. ACM*, vol. 64, no. 7, p. 101–108, jun 2021. [Online]. Available: <https://doi.org/10.1145/3465212>
- [7] J. C. Cardona Restrepo and R. Stanojevic, “A history of an internet exchange point,” *ACM SIGCOMM Computer Communication Review*, vol. 42, no. 2, pp. 58–64, 2012.
- [8] —, “Ixp traffic: a macroscopic view,” in *Proceedings of the 7th Latin American Networking Conference*, 2012, pp. 1–8.
- [9] V. Giotsas, S. Zhou, M. Luckie, and K. Claffy, “Inferring multilateral peering,” in *Proceedings of the ninth ACM conference on Emerging networking experiments and technologies*, 2013, pp. 247–258.
- [10] G. Nomikos, P. Sermpezis, and X. Dimitropoulos, “Re-mapping the internet: Bring the ixps into play: [www.inspire.edu.gr/ixp-map](http://www.inspire.edu.gr/ixp-map),” in *2017 IEEE Conference on Computer Communications Workshops (INFOCOM WKSHPS)*. Atlanta, GA, USA: IEEE, 2017, pp. 910–915.

- [11] C. D. Meyer, “Stochastic complementation, uncoupling markov chains, and the theory of nearly reducible systems,” *SIAM review*, vol. 31, no. 2, pp. 240–272, 1989.
- [12] Authors, “Source code,” June 2022. [Online]. Available: <https://doi.org/XXX>
- [13] A. Lodhi, N. Larson, A. Dhamdhere, C. Dovrolis, and K. Claffy, “Using peeringdb to understand the peering ecosystem,” *ACM SIGCOMM Computer Communication Review*, vol. 44, no. 2, pp. 20–27, 2014.
- [14] D. Jäger, “Analyzing the time dynamics in ixp datasets.”
- [15] S. Brin and L. Page, “The anatomy of a large-scale hypertextual web search engine,” in *Proceedings of the Seventh International Conference on World Wide Web 7*, ser. WWW7. NLD: Elsevier Science Publishers B. V., 1998, p. 107–117.
- [16] Z. Bar-Yossef and L.-T. Mashiach, “Local approximation of pagerank and reverse pagerank,” in *Proceedings of the 17th ACM Conference on Information and Knowledge Management*, ser. CIKM ’08. New York, NY, USA: Association for Computing Machinery, 2008, p. 279–288. [Online]. Available: <https://doi.org/10.1145/1458082.1458122>
- [17] M. Bastian, S. Heymann, and M. Jacomy, “Gephi: An open source software for exploring and manipulating networks,” in *International AAAI Conference on Weblogs and Social Media*, 2009. [Online]. Available: <http://www.aaai.org/ocs/index.php/ICWSM/09/paper/view/154>
- [18] (2020) Peeringdb topology interactive layout. [Online]. Available: [https://www.irit.fr/PeeringDB\\_viz/pDB\\_topology/](https://www.irit.fr/PeeringDB_viz/pDB_topology/)
- [19] A.-L. Barabási and R. Albert, “Emergence of scaling in random networks,” *science*, vol. 286, no. 5439, pp. 509–512, 1999.
- [20] A. Clauset, C. R. Shalizi, and M. E. Newman, “Power-law distributions in empirical data,” *SIAM review*, vol. 51, no. 4, pp. 661–703, 2009.
- [21] A. Barrat, M. Barthelemy, R. Pastor-Satorras, and A. Vespignani, “The architecture of complex weighted networks,” *Proceedings of the national academy of sciences*, vol. 101, no. 11, pp. 3747–3752, 2004.
- [22] (2020) The caida as organizations dataset. [Online]. Available: <http://www.caida.org/data/as-organizations>
- [23] G. Huston. (2020) How big is that network? [Online]. Available: <https://labs.apnic.net/?p=526>
- [24] W. B. Norton. (2020) The 21st century internet peering ecosystem. [Online]. Available: <https://drpeering.net/core/ch10.2-The-21st-Century-Internet-Peering-Ecosystem.html>

- [25] K. M. Frahm, K. Jaffrès-Runser, and D. L. Shepelyansky, “Wikipedia mining of hidden links between political leaders,” *The European Physical Journal B*, vol. 89, no. 12, pp. 1–21, 2016.
- [26] N. Chatzis, G. Smaragdakis, J. Böttger, T. Krenc, and A. Feldmann, “On the benefits of using a large ixp as an internet vantage point,” in *Proceedings of the 2013 Conference on Internet Measurement Conference*, ser. IMC ’13. New York, NY, USA: Association for Computing Machinery, 2013, p. 333–346. [Online]. Available: <https://doi.org/10.1145/2504730.2504746>
- [27] A. Feldmann, O. Gasser, F. Lichtblau, E. Pujol, I. Poese, C. Dietzel, D. Wagner, M. Wichtlhuber, J. Tapiador, N. Vallina-Rodriguez, O. Hohlfeld, and G. Smaragdakis, “The lockdown effect: Implications of the covid-19 pandemic on internet traffic,” in *Proceedings of the ACM Internet Measurement Conference*, ser. IMC ’20. New York, NY, USA: Association for Computing Machinery, 2020, p. 1–18. [Online]. Available: <https://doi.org/10.1145/3419394.3423658>
- [28] T. Böttger, G. Ibrahim, and B. Vallis, “How the internet reacted to covid-19: A perspective from facebook’s edge network,” in *Proceedings of the ACM Internet Measurement Conference*, ser. IMC ’20. New York, NY, USA: Association for Computing Machinery, 2020, p. 34–41. [Online]. Available: <https://doi.org/10.1145/3419394.3423621>
- [29] M. Roughan, W. Willinger, O. Maennel, D. Perouli, and R. Bush, “10 lessons from 10 years of measuring and modeling the internet’s autonomous systems,” *IEEE Journal on Selected Areas in Communications*, vol. 29, no. 9, pp. 1810–1821, 2011.
- [30] J. C. Cardona Restrepo and R. Stanojevic, “A history of an internet exchange point,” *SIGCOMM Comput. Commun. Rev.*, vol. 42, no. 2, p. 58–64, Mar. 2012. [Online]. Available: <https://doi.org/10.1145/2185376.2185384>
- [31] PeeringDB. (2020) Peeringdb. [Online]. Available: <https://www.peeringdb.com>
- [32] PCH. (2020) Packet clearing house ixp datasets. [Online]. Available: <https://www.pch.net/ixp/data>
- [33] D. F. Gleich, “Pagerank beyond the web,” *SIAM Review*, vol. 57, no. 3, pp. 321–363, 2015.
- [34] L. Ermann and D. L. Shepelyansky, “Google matrix analysis of the multi-product world trade network,” *The European Physical Journal B*, vol. 88, no. 4, p. 84, 2015.
- [35] M. Bazzi, M. A. Porter, S. Williams, M. McDonald, D. J. Fenn, and S. D. Howison, “Community detection in temporal multilayer networks, with an

- application to correlation networks,” *Multiscale Modeling & Simulation*, vol. 14, no. 1, pp. 1–41, 2016.
- [36] U. Mori, A. Mendiburu, and J. A. Lozano, “Similarity measure selection for clustering time series databases,” *IEEE Transactions on Knowledge and Data Engineering*, vol. 28, no. 1, pp. 181–195, 2015.
- [37] L. Justin. (2020) Pygomax: Reduced google implementation. [Online]. Available: <https://gitlab.com/xxxx>
- [38] V. D. Blondel, J.-L. Guillaume, R. Lambiotte, and E. Lefebvre, “Fast unfolding of communities in large networks,” *Journal of Statistical Mechanics: Theory and Experiment*, vol. 2008, no. 10, p. P10008, oct 2008. [Online]. Available: <https://doi.org/10.1088%2F1742-5468%2F2008%2F10%2Fp10008>
- [39] Z. Yang, R. Algesheimer, and C. J. Tessone, “A comparative analysis of community detection algorithms on artificial networks,” *Scientific reports*, vol. 6, p. 30750, 2016.
- [40] M. J. Barber, “Modularity and community detection in bipartite networks,” *Physical Review E*, vol. 76, no. 6, p. 066102, 2007.
- [41] L. Feng, Q. Zhao, and C. Zhou, “Improving performances of top-n recommendations with co-clustering method,” *Expert Systems with Applications*, vol. 143, p. 113078, 2020.